Natural and Experimental Evidence of Melt Lubrication of Faults During Earthquakes

Giulio Di Toro,[1]* Takehiro Hirose,[2] Stefan Nielsen,[3] Giorgio Pennacchioni,[1] Toshihiko Shimamoto[2]

Melt produced by friction during earthquakes may act either as a coseismic fault lubricant or as a viscous brake. Here we estimate the dynamic shear resistance (τ_f) in the presence of friction-induced melts from both exhumed faults and high-velocity (1.28 meters per second) frictional experiments. Exhumed faults within granitoids (tonalites) indicate low τ_f at 10 kilometers in depth. Friction experiments on tonalite samples show that τ_f depends weakly on normal stress. Extrapolation of experimental data yields τ_f values consistent with the field estimates and well below the Byerlee strength. We conclude that friction-induced melts can lubricate faults at intermediate crustal depths.

How large is τ_f of faults during earthquakes? Although it is a crucial parameter for understanding the dynamics of seismic rupture, τ_f is virtually inaccessible to seismological methods (*1*–*3*). The interpretation of seismological and geophysical data suggests that many ruptures occur as self-healing pulses (*4*) and that dynamic stress drops are larger than static stress drops (*1*, *5*). Increases in heat flow have not been found near active faults (*6*). These observations can be explained by low τ_f (*4*, *7*). Melt lubrication is a possible cause of low τ_f (*8*–*11*), because solidified, clast-laden, friction-induced melts (pseudotachylytes) decorate some exhumed ancient faults (*12*). However, evidence of melt is not ubiquitous on faults, indicating that other weakening mechanisms may be important, especially in the presence of fluids (*13*–*15*). In addition, a high-viscosity melt might act as a viscous brake, damping seismic slip instead of lubricating (*2*, *11*, *16*, *17*).

Here we estimate τ_f from large exposures of pseudotachylyte-bearing faults and through the experimental production of friction melt on samples from the same natural rock that produced the pseudotachylyte in the fault exposures. Both field and experimental data coherently indicate melt lubrication and low fault strength during earthquakes.

Assuming that most frictional work during faulting is converted into heat (i.e., the energy associated with the creation of new surfaces is negligible) (*2*, *18*), it is possible to determine τ_f from natural pseudotachylytes (*12*). Indeed, if the volume of the pseudotachylyte per unit fault surface, w (in meters), and the displacement d (in meters) accommodated by the fault to produce the melt are known, then (*10*)

$$\tau_f = \rho\left[(1 - \phi)H + c_p(T_i - T_{hr})\right]w/d \quad (1)$$

where $\rho = 2700$ kg m^{-3} is the rock density, $\phi = 0.2$ is the volume ratio of lithic clasts within the pseudotachylyte, $H = 3.28 \times 10^5$ J kg^{-1} is the latent heat of fusion, $c_p = 1180$ J kg^{-1} K^{-1} is the specific heat at constant pressure at 1300 K, and $(T_i - T_{hr}) = 1200$ K is the difference between initial melt temperature and host rock temperature. These values are appropriate for the exhumed strike-slip Gole Larghe fault zone, which crosscuts tonalites of the Adamello batholith (Italian Alps) (*10*, *19*). The fault zone is exposed in glacier-polished outcrops and is composed of about 200 major subparallel faults.

The fault rocks predominantly consist of an association of cataclasites overprinted by pseudotachylytes (*19*). In most of the observed faults, part of the cumulative slip has been accommodated without the production of pseudotachylytes; in such cases, it is not possible to apply Eq. 1. However, a few faults are delineated by pseudotachylyte alone. Pseudotachylytes are distributed along the fault surface and fill injection veins that intrude the host tonalite (Fig. 1, A and B). In these faults, the absence of a precursor cataclasite is confirmed by optical and scanning electron microscope (SEM) investigations. It appears that locally, pseudotachylyte formed during a single seismic rupture that propagated through intact tonalite. The displacement d along these single-event faults was determined from the measured separation of dikes, xenoliths, and mylonites crosscut by the faults (*19*). The volume of the pseudotachylyte per fault surface unit, w, was determined in two ways in

[1]Dipartimento di Geologia, Paleontologia e Geofisica, Università di Padova, 35137, Padova, Italy. [2]Division of Earth and Planetary Sciences, Graduate School of Science, Kyoto University, Kyoto 606–8502, Japan. [3]Research Unit RISSC Istituto Nazionale di Geofisica e Vulcanologia, Roma 1, 00143 Rome, Italy.

*To whom correspondence should be addressed. E-mail: giulio.ditoro@unipd.it

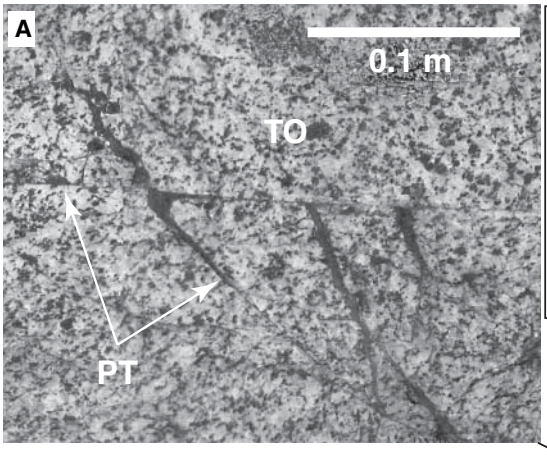

C

Outcrop	Fault displ. mm	PT thickn. mm	Thickn./ displ.	Shear stress MPa
Lobbia 2000_1*	120	0.5	0.0042	18.9
32 _ 2003*	250	2.0	0.0080	36.3
Lobbia 2000_2*	340	1.5	0.0044	20.0
Lobbia 2000_3*	500	2.0	0.0040	18.1
P058 35m vs N*	610	2.0	0.0033	14.9
Lobbia 2000_4*	660	7.0	0.0106	48.1
P040 10m vs N*(AM)	790	6.9	0.0087	39.6
A14_2004 (AM)	1440	5.9	0.0041	18.6

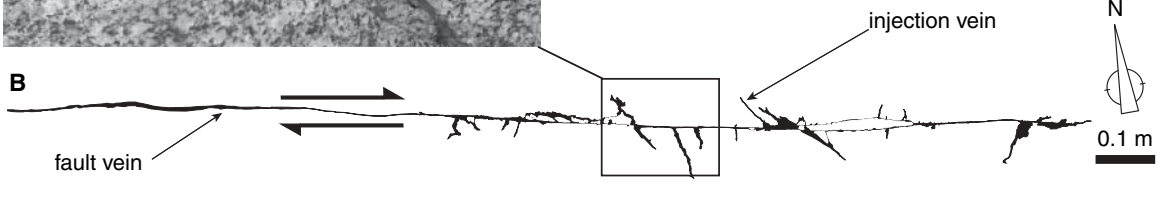

Fig. 1. Field example of pseudotachylyte. (**A**) Pseudotachylytes (PT, black color) decorate the main fault and are locally injected into the tonalitic (TO) host rock. (**B**) Fault profile of a pseudotachylyte-bearing fault. Note the variation in thickness of the pseudotachylyte along strike. (**C**) Table of field data. Asterisks indicate data published in (*10*); AM, area method. Dynamic shear stress τ_f was estimated from Eq. 1 using the ratio of observed PT thickness and fault offset.

outcrops orthogonal to fault dip. For thin, continuous fault veins of constant thickness and free of injection veins, we measured w as the average pseudotachylyte thickness along the studied fault segment [following the method described by Sibson (*12*)]. For thick and complex pseudotachylyte-bearing vein networks (Fig. 1A), we determined w by dividing the outcrop area occupied by the melt (including the pseudotachylyte in the fault vein as well as in injection veins and dilation jogs) (Fig. 1B) for the length of the fault profile ("area method") (*10*). From the w/d values of single-event pseudotachylyte of the Gole Larghe Fault, Eq. 1 yields τ_f between 14.9 and 48.1 MPa (Fig. 1C).

In the Gole Larghe fault, seismic slip (pseudotachylyte production) occurred at temperatures of 250 to 300°C and at depths of 9 to 11 km (*20*). During faulting, a low pore fluid pressure can be assumed on the basis of several microstructural observations (*10*). On the other hand, the production of pseudotachylytes indicates relatively dry conditions, because the presence of fluids activates other weakening mechanisms (e.g., thermal pressurization by pore fluids) that might prevent the onset of bulk frictional melting (*13*). Assuming low fluid pressures and a stress tensor in agreement with strike-slip faulting (*10*, *21*), the effective stress normal to the fault at a depth of 10 km (for a rock density of 2600 kg m^{-3}) is between 112 MPa (hydrostatic pore pressure) (*10*) and 182 MPa (no pore pressure).

Four high-velocity rock friction experiments were conducted in a rotary shear apparatus (*22*). In each experiment, we used a pair of solid cylinders (22.3 mm in diameter and ~23 mm in length) of tonalite from the host rock of the Gole Larghe fault zone. A different normal load σ_n was applied during each experiment (5, 10, 15, and 20 MPa). The samples were subjected to a sudden step in rotation velocity from 0 rpm (velocity of 0 m s^{-1}) to 1500 rpm (which corresponds to an equivalent slip velocity of 1.28 m s^{-1}) (Fig. 2) (*22*). The imposed equivalent slip velocity is within the range of seismic slip rates (1 to 3 m s^{-1}) estimated for natural earthquakes (*1*, *2*, *4*). Specimens were jacketed with a 1-mm-thick aluminum ring to avoid sample destruction by thermal fracturing (*23*). This sample preparation allowed the application of σ_n up to 20 MPa, which is 1 order of magnitude larger than in previous shear melting experiments (*22*, *24*). The area of the aluminum ring in contact with the sliding surface was rapidly consumed because of the relatively low melting temperature of aluminum (660°C), compared with that of the dominant tonalite-forming minerals [>1000°C (*25*, *26*)]. Under the relatively high applied σ_n, runs lasted from 4 to 8 s and displacements reached a few meters, in contrast with the several tens of seconds and tens of meters achieved during previous studies (*22*, *24*). The durations of our experiments are comparable to the typical rise time of large earthquakes (*2*, *4*).

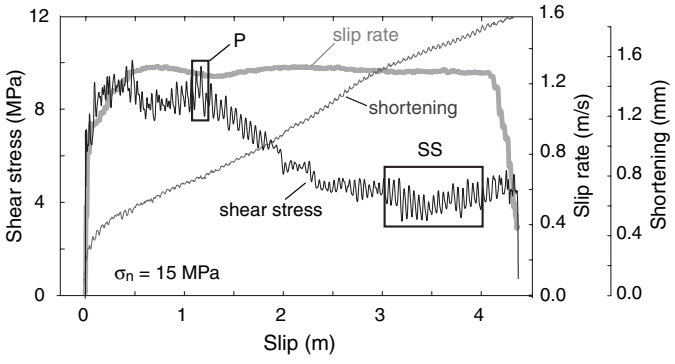

Fig. 2. Experimental results for tonalite at a slip rate of 1.28 m s^{-1} and normal stress of 15 MPa. Boxes P and SS indicate the displacement intervals used to determine peak and steady-state shear stress, respectively, plotted in Fig. 4A.

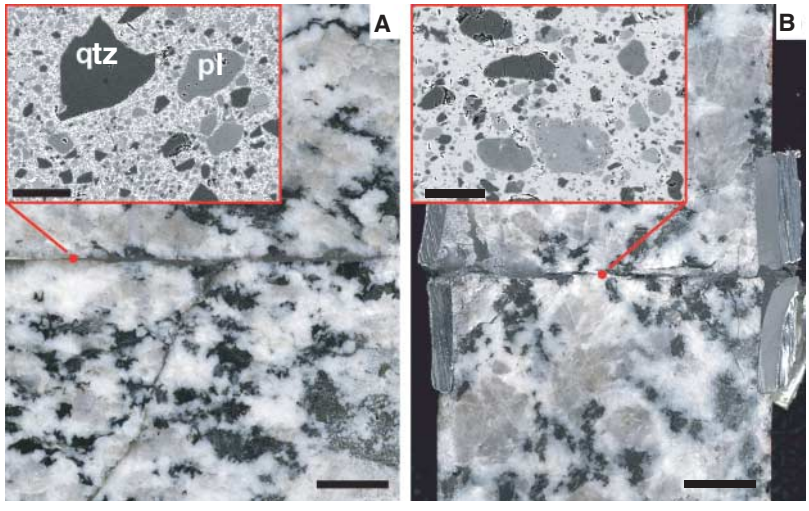

Fig. 3. Comparison between (**A**) natural and (**B**) experimental pseudotachylyte. The insets are SEM back-scatter images of the pseudotachylyte (inset scale bars, 50 μm). Pseudotachylytes consist of quartz (qtz) and plagioclase (pl) clasts suspended within a biotite (bright white) microlitic matrix in natural pseudotachylyte (A) or in a glassy matrix in artificial pseudotachylyte (B). In (B), the aluminum external ring is bent toward the outside and separated by a thin but continuous melt layer. The bulge to the right is epoxy. Scale bars, 5 mm.

During the experiments, friction-induced melt was produced along the sliding surface and largely extruded from the sample assembly. Such melt extrusion resembles what happens in natural faults, where most of the melt has been injected from the sliding surface of the fault where it was produced (i.e., fault vein) into lateral veins (i.e., injection veins) or pull-apart regions (Fig. 1, A and B). Some melt still remained along the sliding surface at the end of the experiment, and this remaining melt formed a continuous layer of artificial pseudotachylyte that resembled natural pseudotachylytes of the Gole Larghe fault (Fig. 3). Pseudotachylyte consists of quartz and plagioclase clasts immersed in a microlitic (natural pseudotachylyte) (Fig. 3A) or glassy (artificial pseudotachylyte) (Fig. 3B) matrix. Microlites are absent in artificial pseudotachylytes, because the cooling of the melt to laboratory room temperature (20°C) is more rapid than in the Gole Larghe fault, where the host rock temperature was 250 to 300°C (*20*).

During the experiments, the shear stress increased up to a peak value achieved after ~1.0 m of sliding (Fig. 2, box marked P). This initial fault strengthening reflects the formation and shearing of discontinuous melt patches between the rock surfaces (*22*). After the peak value, the shear stress gradually decreased (transient stage), usually over 1 to 2 m of slip, toward a steady-state shear stress (Fig. 2, box marked SS). Melt was squeezed out from the specimen throughout the experiment, starting from the transient stage (*26*). During the steady-state stage, the specimen shortened at a constant rate of ~0.5 mm s^{-1} as melt was produced and evacuated (Fig. 2). Thus, steady-state shear stress is achieved in the presence of the following: (i) a continuous film of melt wetting the sliding surface (Fig. 3B) and (ii) steady evacuation of melt, confirmed by the constant shortening rate of the sample.

In a viscous regime, defining the standard friction coefficient as $\mu = \tau_f/\sigma_n$—as in the case

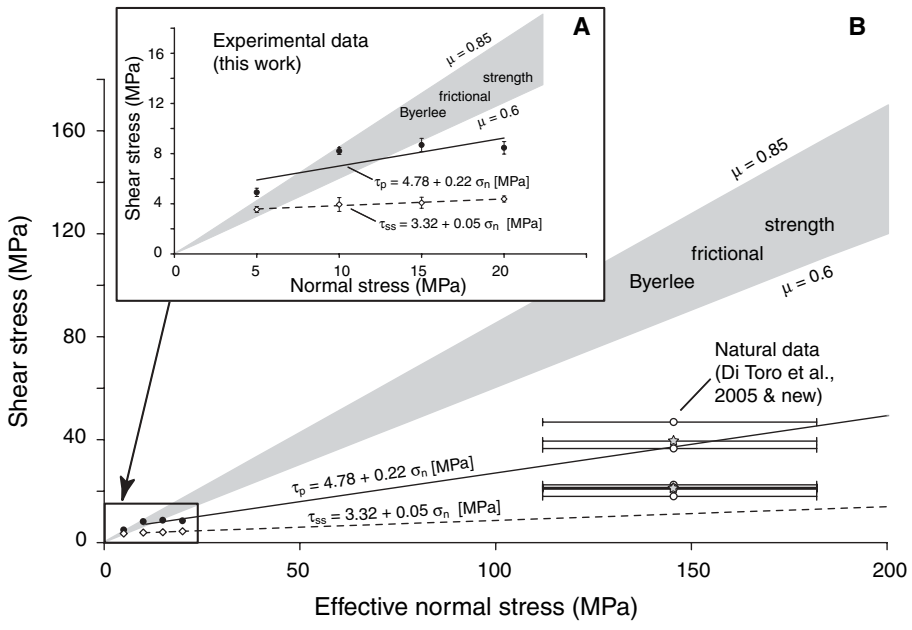

Fig. 4. Shear stress versus effective normal stress for (**A**) experimental data and (**B**) natural data, compared with Byerlee's frictional strength for tonalite. Solid circles and open diamonds are experimental values for peak shear stress and steady-state shear stress (Fig. 2), respectively; open circles and open stars are field data estimates according to Eq. 1. Open stars indicate estimates by means of the area method. Experimental data have vertical error bars (SD) due to the slight oscillations in shear stress with displacement (Fig. 2). Field data have a large range of effective normal stress (as indicated by the horizontal error bars) due to the poorly constrained pore pressure at the time of seismic faulting. The solid line is the best linear fit for the peak shear stress data; the dashed line is the best linear fit for the steady-state shear stress data. Most field data lay within the dynamic shear strength curves extrapolated from the experimental data, well below Byerlee's friction curves (plotted in gray as a reference for $0.6 < \mu < 0.8$).

of solid friction—is misleading (*11*, *22*). Instead, we represent τ_f as a function of σ_n, and the simple form $\tau_f = \alpha + \mu_{eff}\,\sigma_n$ reasonably fits the data, where α is the intercept at zero normal stress and μ_{eff} is an effective friction coefficient (Fig. 4A). For peak shear stress (black line), $\tau_f = 4.78 + 0.22\sigma_n$ (in MPa), whereas for steady-state shear stress (dashed line), $\tau_f = 3.32 + 0.05\sigma_n$ (in MPa). It appears that shear stress is weakly sensitive to σ_n, whereas in a purely viscous regime, resistance to slip is independent of the normal stress (*11*). In the studied natural faults, the sliding surfaces are wetted by a continuous melt layer, which is one of the two conditions satisfied during the steady-state stage in the experiments. However, the τ_f deduced for the natural faults is an average value integrated over the entire slip event (i.e., strengthening and weakening), so it is expected to lie between the peak and steady-state shear stress.

The best-fit curves for shear stress determined in the lab (Fig. 4A) have been extrapolated to crustal conditions at depths of 10 km and are in reasonable agreement with the field data (Fig. 4B). These findings show that shear strength is low in the presence of melts during seismic slip. The field data indicate that τ_f is lower than that for Byerlee's frictional strength (*27*). The experimental data also indicate that τ_f is low and has a slight dependence on normal stress. This is a clear deviation from Byerlee's law (Fig. 4A) and suggests melt lubrication. Overall, the experimental and field estimates of τ_f follow nearly the same dynamic strength curve, indicating good agreement between laboratory and field data and that dynamic fault strength is well below that assumed for a typical Byerlee's frictional law.

Although the abundance of pseudotachylytes in nature is still a debated issue, friction-induced melts are easily produced in the laboratory. The effects of melt lubrication on the fault surface must be considered in some earthquake rupture models.

References and Notes

1. H. Kanamori, T. H. Heaton, in *Geocomplexity and the Physics of Earthquakes*, J. Rundle, D. L. Turcotte, W. Klein, Eds. (Geophys. Res. Monogr. Ser. **120**, American Geophysical Union, Washington, DC, 2000), pp. 147–163.
2. C. H. Scholz, *The Mechanics of Earthquakes and Faulting* (Cambridge Univ. Press, New York, ed. 2, 2002).
3. The τ_f value cannot be determined by seismological methods unless a difficult reconstruction of rake rotation is possible. In this case, the absolute level of stress is accessible as shown in (*28*).
4. T. H. Heaton, *Phys. Earth Planet. Inter.* **64**, 1 (1990).
5. M. Bouchon, *J. Geophys. Res.* **102**, 11731 (1997).
6. J. N. Brune, T. L. Henyey, R. F. Roy, *J. Geophys. Res.* **74**, 3821 (1969).
7. G. Zhang, J. R. Rice, *Bull. Seism. Soc. Am.* **88**, 1466 (1998).
8. J. G. Spray, *J. Geophys. Res.* **98**, 8053 (1993).
9. J. G. Spray, *Geophys. Res. Lett.* **32**, L07301 (2005).
10. G. Di Toro, G. Pennacchioni, G. Teza, *Tectonophysics* **402**, 3 (2005).
11. Y. Fialko, Y. Khazan, *J. Geophys. Res.* **110**, 10.1029/2005JB003869 (2005).
12. R. H. Sibson, *Geophys. J. R. Astron. Soc.* **43**, 775 (1975).
13. R. H. Sibson, *Nat. Phys. Sci.* **243**, 66 (1973).
14. E. E. Brodsky, H. Kanamori, *J. Geophys. Res.* **106**, 16357 (2001).
15. G. Di Toro, D. L. Goldsby, T. E. Tullis, *Nature* **427**, 436 (2004).
16. Y. Koizumi, K. Otsuki, A. Takeuchi, H. Nagahama, *Geophys. Res. Lett.* **31**, L21605 (2004).
17. Laboratory experiments that reproduce in situ conditions during earthquakes may yield a definitive answer, but reproducing the extreme deformation conditions of earthquakes represents an overwhelming technical challenge, mainly attributal to severe thermal fracturing of rock specimens (*23*).
18. Indeed, this is the case of the studied pseudotachylytes, because estimated fracture surface energy is less than 2% of the energy exchanged as heat (*29*).
19. G. Di Toro, G. Pennacchioni, *Tectonophysics* **402**, 54 (2005).
20. G. Di Toro, G. Pennacchioni, *J. Struct. Geol.* **26**, 1783 (2004).
21. R. H. Sibson, *Nature* **249**, 542 (1974).
22. T. Hirose, T. Shimamoto, *J. Geophys. Res.* **110**, B05202 (2005).
23. Y. Ohtomo, T. Shimamoto, *Struct. Geol.* **39**, 135 (1994) (in Japanese with English abstract).
24. A. Tsutsumi, T. Shimamoto, *Geophys. Res. Lett.* **24**, 699 (1997).
25. The mineral composition of the tonalite bounding the Gole Larghe Fault zone is 48% plagioclase (~1200°C), 29% quartz (~1700°C), 17% biotite (~650°C), and 6% K-feldspar (~1150°C) (*20*). Individual melting temperature are in parentheses.
26. The friction-induced melt appears after ~0.5 m of sliding, and it is squeezed out from the sliding surface because of the large σ_n exerted (Movie S1). At this initial stage, the aluminum rings were already weakened and bent toward the outside by the starting melt extrusion (Fig. 3B). We conclude that the aluminum rings were not in contact during the experiment—with the exception of the initial sliding phase—and mechanical data are not affected by the frictional strength of the external aluminum ring. This was confirmed by specimen investigation after the experiments, which showed that the two opposite aluminum rings were separated by a thin and continuous tonalitic melt layer (Fig. 3B). Other experiments indicated that the selected shape of the sample (solid instead of hollow shaped) did not affect the mechanical data, because peak and steady-state shear stress are similar for both type of specimens, although shear stress versus displacement curves might be slightly different (fig. S1), as discussed in (*11*).
27. J. D. Byerlee, *Pure App. Geophys.* **116**, 615 (1978).
28. M. Guatteri, P. Spudich, *Bull. Seismol. Soc. Am.* **88**, 777 (1998).
29. L. Pittarello, G. Di Toro, A. Bizzarri, J. Hadizadeh, G. Pennacchioni, *EOS Trans. AGU* **86**, S41B-0997 (2005).

30. We thank the Japanese Center of Excellence for the 21st Century program for sustaining G.D.T.'s visit in Kyoto, the Progetto di Ateneo 2003 (Università di Padova) for covering SEM costs, and a grant from Istituto Nazionale di Geofisica e Vulcanologia for covering the field expenses. We thank Y. Fialko and A. Rempel for comments and A. Novello, L. Tauro, and S. Castelli for sample preparation and photos used in Fig. 3.

Supporting Online Material

www.sciencemag.org/cgi/content/full/311/5761/647/DC1
Fig. S1
Movie S1

5 October 2005; accepted 30 December 2005
10.1126/science.1121012

Natural and Experimental Evidence of Melt Lubrication of Faults During Earthquakes

Giulio Di Toro *et al.*

Science **311**, 647 (2006);
DOI: 10.1126/science.1121012